2022 EAGE ANNUAL
83RD CONFERENCE & EXHIBITION
MADRID I SPAIN

STEPPING TOWARDS AUTOMATED MULTISENSOR NOISE ATTENUATION GUIDED BY DEEP LEARNING

B. Farmani[1], Y. Pal[1], M.W. Pedersen[1], E. Hodges[1]

[1] PGS

Summary

Despite technological advancements in marine seismic multisensor acquisition and processing, noise attenuation remains a fundamental step in the early processes for producing high-quality upgoing pressure wavefield data. If we assume the main shortcoming of traditional methods is in the noise detection step, deep learning can be used in only the detection step and the selected noise attenuation engine can be automatically guided by the deep learning noise classification. We have created different deep learning models to detect a variety of noise types present in both marine hydrophone and geophone records. These models are used to automatically classify the samples in the noise attenuation workflows and pass the samples to the appropriate noise attenuation steps. Targeted noise detection lets us perform a better targeted noise attenuation with appropriate levels of harshness without undue concern over possible signal loss. Models can also be used at any step of the processing to classify the samples in both hydrophone and geophone records. The improvement in noise attenuation and its impact on the P-UP generation is presented for a real dataset. The advantages to turnaround and quality that arise from the use of these workflows are discussed.

Stepping Towards Automated Multisensor Noise Attenuation Guided by Deep Learning

Introduction

Despite technological advancements in marine seismic multisensor acquisition and processing, noise attenuation remains a fundamental step in the early processes for producing high-quality upgoing pressure wavefield (P-UP) data. As the nature and level of noise often varies during a survey, the traditional approach of using one fixed set of parameters in the selected noise attenuation algorithm is often sub-optimal. For example, on hydrophone records the level of swell noise can vary significantly throughout a survey. For records with a low level of swell noise, a mild noise attenuation is needed, but if there are records contaminated with a much higher level of swell noise, a harsher noise attenuation should be applied to only those records. In traditional algorithms, such as FX filters, we usually rely on amplitude-based statistical methods to locate the noisy samples. However, it is obvious that such approaches can, for example, mistake isolated high amplitude signal for noise or spatially wide bands of noise as signal.

The entire process of swell noise attenuation can be replaced by deep learning methods (e.g., Zhao et. al., 2019). Alternatively, if we assume the main shortcoming of traditional methods is in the noise detection step, deep learning can be used in only the detection step (e.g., Farmani and Pedersen, 2020a and 2020b). One advantage of using deep learning for noise detection is that it has been shown it can reliably classify the samples. For example, high amplitude isolated signal and wide bands of noise do not present a problem for the classification. Therefore, the selected noise attenuation engine can be automatically guided by the deep learning noise classification. This has provided the flexibility to progressively increase the harshness of the noise attenuation without undue concern over possible signal loss. Other types of noise such as turn noise, current noise, door wash noise and impact spikes are commonplace in hydrophone records. Such type of noise may need an additional dedicated workflow. Therefore, we have extended Farmani and Pedersen (2020b) methodology to detect, distinguish and attenuate the above types of hydrophone noise.

We have created different deep learning models to detect a variety of noise types present in both marine hydrophone and geophone records. These models are used to automatically classify the samples in the noise attenuation workflows and pass the samples to the appropriate noise attenuation steps. Targeted noise detection lets us perform a better targeted noise attenuation with appropriate levels of harshness. Models can also be used at any step of the processing to classify the samples in both hydrophone and geophone records. The improvement in noise attenuation and its impact on the P-UP generation is presented for a real dataset.

Methodology

The workflows consist of three main elements: deep learning classification networks, FX deconvolution filters and FX projection filters. We use the U-Net network to classify the samples. U-Net is a convolutional network developed by Ronneberger et al. (2015) for the classification of medical images. This network has been used in the seismic industry to address different classification and regression problems. Depending on the type and frequency of the targeted noise, we use different FX filters with different pre-defined parameters. In general, FX filters are wrapped with a classification network and the harshness of the filtering progressively increases as workflow advances further. In this way we can further attenuate any remnant noise in each successive step whilst reducing the chance of signal loss. The workflows are automated in the sense that no user parameterization is required since the workflows decide by themselves where they need to remove more noise and which parameters should be used.

The hydrophone workflow uses three U-Net networks (Figure 1a). All hydrophone networks have four down-sampling and up-sampling steps, and there are 16 filters for the first encoder. Since noise on the hydrophone records is generally confined to lower frequencies, input traces to the networks are down-sampled. The networks have three or four output classes: signal, noise, signal-and-noise, and mask.

Mask represents the zero samples. For more general detailed information about the network and its performance refer to Farmani and Pedersen (2020a). All models were trained using a combination of real data from different surveys. Firstly, a U-Net network (U-Net H1 in Figure 1a) was trained to detect swell, turn and door wash noises with frequencies above 10 Hz. The classified noisy samples are further subclassified into two groups of wide-band and local noise and are processed separately. Wide-band noise is defined as noise spreading on more than dozens of traces for more than couple of seconds. A second U-Net network (U-Net H2 in Figure 1a) was trained to detect the same types of noises but with frequencies below 10 Hz. This network is used twice in the hydrophone workflow. A third U-Net network (U-Net H3 in Figure 1a) was trained to find the possible signal leakage in the energy attenuated in the previous step which is added back to the signal before the process moves on to the next step. At the end of the workflow a map is created containing the percentage of noisy samples for each trace which gives a quick overview of the performance of the network for quality control (QC). Note that this QC map can be generated for any input at any stage if required.

The geophone workflow uses two U-Net networks (Figure 1b). Both networks have four down-sampling and up-sampling layers like the hydrophone. However, the first encoder with 16 filters is applied after the first down-sampling. Both geophone networks were trained using synthetic and real data from cold-water surveys. One network detects the noise with frequencies above 30 Hz (U-Net G1 in Figure 1b) and the other one detects noise with frequencies below 30 Hz (U-Net G2 in Figure 1b). A similar QC map as for the hydrophone is also generated for the geophone at the end of the workflow.

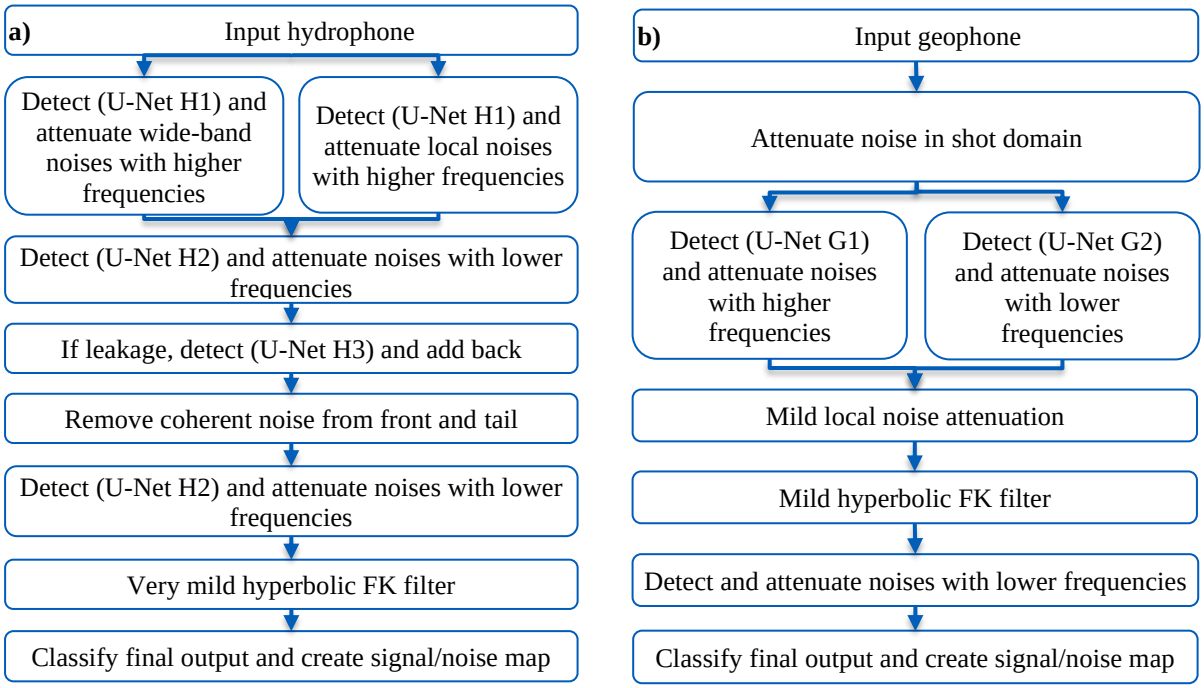

Figure 1: flowcharts of the noise attenuation workflows for a) hydrophone and b) geophone records.

Both hydrophone and geophone workflows have been extensively tested on different surveys and consistently produce very encouraging results. Note that even though workflows have been developed to be generic, it is still possible to change the embedded noise attenuation engine or its parameterisation if needed. Alternatively, an additional noise attenuation pass can be applied if the final QC map shows any localized residual noise remaining in the data.

Example

Data selected for this example were acquired using a dual-sensor streamer in the North Sea. Both hydrophone and geophone components were processed using the workflows described above. Figure 2a shows the hydrophone shot gathers before noise attenuation. Note the strong swell noise on the last two shot gathers. All noise was effectively attenuated (Figure 2b) without any evidence of signal leakage in

the attenuated noise model (Figure 2c). The coherent dipping energy evident in Figure 2c was removed by the FK filters in the workflow. Figure 3a shows the geophone records for the same shot gathers. The dominant noise on the geophone records is mechanical vibrations associated with attached devices. Swell noise is also present on the third shot gather. The geophone noise attenuation workflow was able to remove majority of the noises (Figure 3b) without any visible signal loss (Figure 3c). Our experience so far shows that the presented workflows are in general able to remove more noise from both hydrophone and geophone records compared to conventional user designed workflows. This is because more cascaded filters exist in the workflow than what a user would in general design using one or a few test lines. Since we identify the noisy samples using U-Net networks before the application of the filters, each filter is triggered only when it is needed and hence, the signal preservation will be naturally guaranteed for the samples that do not contain the noise targeted in each step of the workflows.

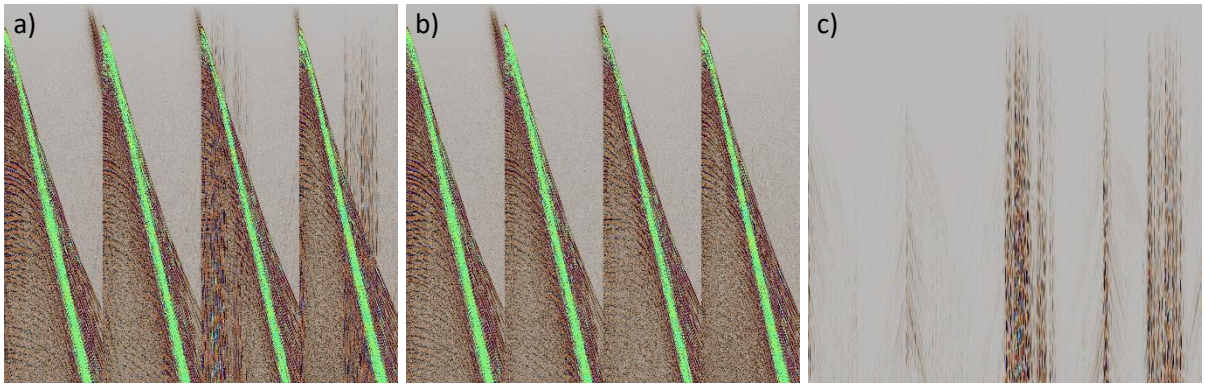

Figure 2: Shot gather examples of hydrophone records a) before and b) after the noise attenuation. c) noise attenuated by the workflow.

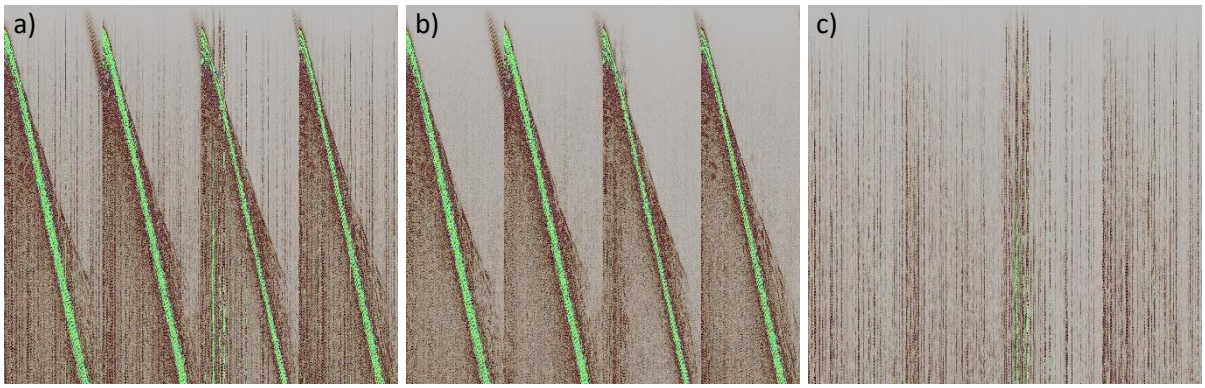

Figure 3: Shot gather examples of geophone records a) before and b) after the noise attenuation. c) noise attenuated by the workflow. Displays have 20-25 Hz Ormsby lowcut filter which was used as low frequency compensation in P-UP generation.

Cleaner hydrophone and geophone records naturally produce a cleaner P-UP with a better signal to noise ratio. In addition, clean data also helps the interpolation algorithm to produce better interpolated traces which are usually needed to satisfy the Nyquist sampling criterion for P-UP generation. In Figure 4 we show a comparison between a P-UP QC stacked section from the same line generated using legacy noise attenuation (Figure 4a) and the equivalent stack created using the presented noise attenuation workflows (Figure 4b). The stacked section has a bandpass filter of 31-62 Hz applied which covers the frequencies of the first hydrophone notch for this acquisition such that the majority of the signal is derived from the geophone. From inspection of weaker amplitude reflectors, we see that P-UP generated after the presented noise attenuation workflows (Figure 4b) has better signal to noise ratio compared to the legacy stack (Figure 4a).

Conclusions

Noise attenuation workflows have been designed for both marine hydrophone and geophone records where different U-Net networks have been used to classify the noisy samples at several steps of the workflows. In each step a combination of FX filters has been designed to attenuate the noise for the samples identified as noisy by U-Net networks. In the hydrophone workflow one U-Net network is also used to detect any signal leakage in the noise model which is then added back to the records. U-Net networks also generate QC maps for performance assessment. Both workflows have shown encouraging performance without any user interaction and can, in general, produce consistently cleaner hydrophone and geophone records compared to what could traditionally be achieved. We also demonstrate that this cleaner data has a direct measurable impact on the P-UP quality.

The advantages to turnaround and quality that arise from the use of these workflows are abundantly clear. Firstly, under most circumstances there is now no need for a denoise testing phase ahead of production. Secondly, the automation of the noise classification means the user is no longer required to pick out subsets of the dataset for additional specific harsher noise attenuation workflows. Finally, the successful accurate classification has significant benefits to both the quality of the output and the time the user spends reviewing QC displays as the user is quickly directed towards any ambiguities.

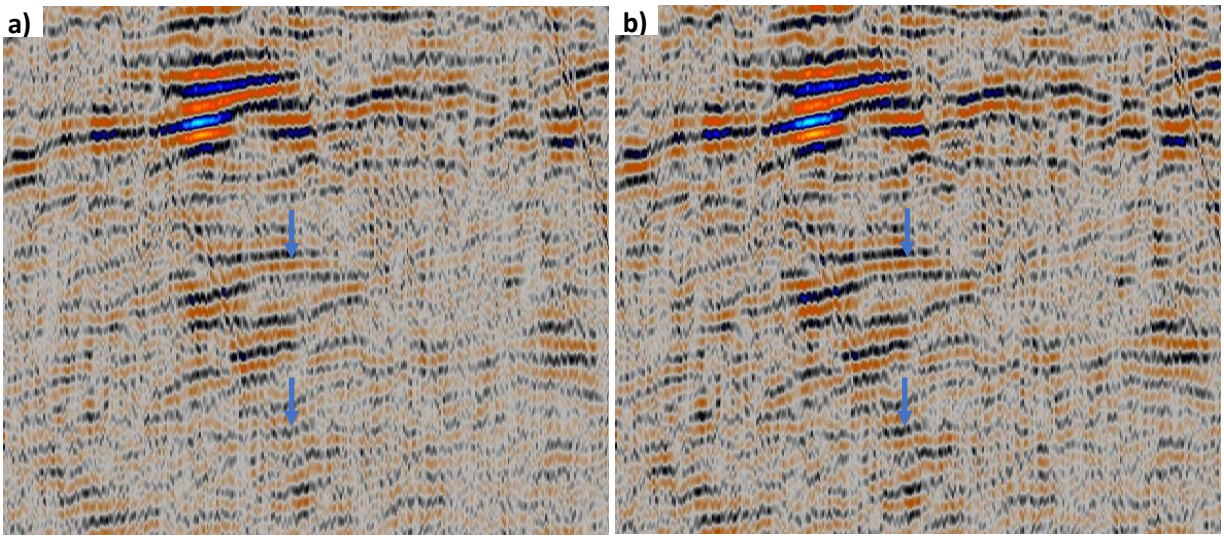

Figure 4: P-UP stack 31-62 Hz with a) legacy noise attenuation and b) deep learning guided noise attenuation.

Acknowledgements

We would like to thank PGS for the permission to publish these results.

References

Farmani, B. and Pedersen, M.W. [2020a] Application of a convolutional neural network to classification of swell noise attenuation. *SEG Technical Program Expanded Abstracts*: 2868-2872.

Farmani, B. and Pedersen, M.W. [2020b] Application of Convolutional Neural Network in Automated Swell Noise Attenuation. *EAGE 2020 Annual Conference & Exhibition Online*, Dec 2020, Volume 2020, p.1-5.

Ronneberger, O., Fischer, P. and Brox, T. [2015] U-Net: Convolutional Networks for Biomedical Image Segmentation. *Medical Image Computing and Computer-Assisted Intervention (MICCAI)*, Springer, LNCS, Vol.9351: 234-241.

Zhao, X., Lu, P., Zhang, Y., Chen, J. and Li, X. [2019] Swell-noise attenuation: A deep learning approach: *The Leading Edge*, 38, 934-942.